Rabi-coupling-driven motion of a soliton in a Bose-Einstein condensate

Sh. Mardonov,[1,2] M. Modugno,[3,4] E. Ya. Sherman,[1,3] and B. A. Malomed[5]

[1]*Department of Physical Chemistry, University of the Basque Country UPV/EHU, 48080 Bilbao, Spain*
[2]*Samarkand State University, 140104 Samarkand, Uzbekistan*
[3]*IKERBASQUE, Basque Foundation for Science, Bilbao, Spain*
[4]*Department of Theoretical Physics and History of Science, University of the Basque Country UPV/EHU, 48080 Bilbao, Spain*
[5]*Department of Physical Electronics, School of Electrical Engineering, and Center for Light-Matter Interaction, Tel Aviv University, Tel Aviv 69978, Israel*

(Received 2 November 2018; published 15 January 2019)

We study the motion of a self-attractive Bose-Einstein condensate with pseudospin $\frac{1}{2}$ driven by a synthetic Rabi (Zeeman-like) field. This field triggers the pseudospin dynamics resulting in a density redistribution between its components and, as a consequence, in changes of the overall density distribution. In the presence of an additional external potential, the latter produces a net force acting on the condensate and activates its displacement. As an example, here we consider the case of a one-dimensional condensate in a random potential.

DOI: 10.1103/PhysRevA.99.013611

I. INTRODUCTION

The dynamics of self-interacting quantum matter in a random potential is a topic of a great significance [1–3]. Adding a spin degree of freedom and spin-orbit coupling (SOC) considerably extends the variety of patterns featured by these settings. The resulting coupled spin and mass density motion is one of the most interesting manifestations of the underlying SOC [4], where the particle's spin is directly coupled to its momentum, and the spin evolution naturally drives changes in the particle's position, for both solid-state [5–7] and cold-atom realizations alike [8,9]. The same mechanism may determine the motion of matter-wave solitons [10].

Taking a self-attractive two-component Bose-Einstein condensate (BEC), which constitutes a pseudospin-$\frac{1}{2}$ system, as an example, we show here that such a mutual dependence of pseudospin and position can occur even without SOC provided that the BEC symmetry with respect to the spin rotations is lifted by particle-particle interactions. This effect occurs in generic situations when the inter- and intraspecies couplings are not equal, resulting in the non-SU(2)-symmetric nonlinearity, as it is often the case for mean-field interaction in binary BECs. Then the pseudospin-dependent force driving the BEC may appear as a joint result of the Rabi (Zeeman) coupling acting on the atomic hyperfine states, and thus affecting the BEC shape, and an external random potential into which the BEC is loaded.

II. MODEL AND MAIN PARAMETERS

We consider a quasi-one-dimensional condensate in the presence of a synthetic Rabi (Zeeman) field applied along the x direction and of a spin-diagonal random potential $U(x)$. The two-component pseudospinor wave function $\boldsymbol{\psi}(\mathbf{x}) \equiv [\psi_1(\mathbf{x}), \psi_2(\mathbf{x})]^{\mathsf{T}}$ [T stands for transpose and $\mathbf{x} \equiv (x, t)$] obeys two Gross-Pitaevskii equations ($\nu, \nu' = 1, 2$)

$$i\partial_t\psi_\nu(\mathbf{x}) = \left[-\frac{1}{2}\partial_{xx} + U(x)\right]\psi_\nu(\mathbf{x}) - [g|\psi_\nu(\mathbf{x})|^2 + \tilde{g}|\psi_{\nu'}(\mathbf{x})|^2]\psi_\nu(\mathbf{x}) + \frac{\Delta}{2}\psi_{\nu'}(\mathbf{x}), \tag{1}$$

where Δ is the Zeeman splitting and $g, \tilde{g} > 0$ are the interatomic interaction constants. Units are chosen such that $\hbar = M = N = 1$, where M is the particle mass and N is the norm. In the absence of the random potential, this model has been studied extensively in nonlinear optics of dual-core fibers (albeit in the time domain), where $\tilde{g} = 0$, with Δ corresponding to the coupling between the fibers [11,12] and in Rabi-coupled BECs [13–16], where both g and $\tilde{g}$ are present. An implementation with small random variations of $\Delta(t)$ has been considered in Ref. [17].

Here we describe the system evolution by means of the density matrix $\boldsymbol{\rho}(\mathbf{x}) \equiv \boldsymbol{\psi}(\mathbf{x})\boldsymbol{\psi}^{\dagger}(\mathbf{x})$ and obtain observables by corresponding tracing. We characterize the condensate motion by the center-of-mass position $X(t)$,

$$X(t) = \mathrm{tr}\int_{-\infty}^{\infty} x\boldsymbol{\rho}(\mathbf{x})dx, \tag{2}$$

and the spin components $\sigma_i(t)$ (here $i = x, y, z$) as

$$\sigma_i(t) = \mathrm{tr}\int_{-\infty}^{\infty} \hat{\sigma}_i\boldsymbol{\rho}(\mathbf{x})dx, \tag{3}$$

where $\hat{\sigma}_i$ are the Pauli matrices. For a general description of the spin state we introduce its squared length $P(t) = \sum_i \sigma_i^2(t)$. When the two spinor components are linearly dependent, $P(t) = 1$, the spin state is pure and it is located on the Bloch sphere.

The characteristic size of relatively high-density domains of the BEC is given by the normalized participation ratio $\zeta(t)$,

$$\zeta(t) \equiv \frac{1}{3}\left[\int_{-\infty}^{\infty} |\boldsymbol{\psi}(\mathbf{x})|^4 dx\right]^{-1}. \quad (4)$$

The prefactor $\frac{1}{3}$ is chosen for consistency with the BEC width $w(t) = [N_1(t)w_1^2(t) + N_2(t)w_2^2(t)]^{1/2}$. The latter characterizes its total spread, with

$$w_\nu^2(t) \equiv \int_{-\infty}^{\infty} x^2 \left|\psi_\nu^2(\mathbf{x})\right| \frac{dx}{N_\nu(t)}, \quad N_\nu(t) \equiv \int_{-\infty}^{\infty} \left|\psi_\nu^2(\mathbf{x})\right| dx. \quad (5)$$

Here $w_\nu(t)$ is the component width and $N_\nu(t)$ is the corresponding fraction of atoms with $N_1(t) + N_2(t) = 1$.

III. SOLITON EVOLUTION

A. Free-space spin rotation and broadening

Here we present the analysis, which can be obtained also by summarizing the results known in the general theory of Rabi solitons in different systems, by expressing them in terms of the pseudospin-$\frac{1}{2}$ BEC. To focus on the most fundamental effects, we consider first a realization maximally different from the SU(2)-symmetric Manakov-like case [18], assuming $\tilde{g} = 0$ (the role of this cross coupling will be discussed later on). The Zeeman field couples the spinor components and leads to evolution of $\sigma_i(t)$ defined by Eq. (3). This spin rotation causes a population redistribution between components of the BEC spinor and therefore modifies its self-interaction energy. As a result, the Zeeman coupling and self-interaction energies become mutually related and the shape of the soliton changes accordingly. In order to better understand this process and for the qualitative analysis, we begin with the free motion where $U(x) \equiv 0$.

Since the effect of the Zeeman field depends on the initial spin configuration, for definiteness and simplicity, here we consider an initial state with $\sigma_z(0) = 1$. At $\Delta = 0$, a stationary solution of Eq. (1) is

$$\psi_1(\mathbf{x}) = e^{-i\mu t}\frac{\text{sech}(x/w_0)}{\sqrt{2w_0}}, \quad \psi_2(\mathbf{x}) = 0, \quad (6)$$

where $w_0 = 2/g$ determines the energy scale,[1] fixing the value of the chemical potential to $\mu = -g^2/8$. We indicate the relevant timescale as $T_\mu \equiv 1/|\mu|$, similar to the expansion time of a noninteracting wave packet of the width w_0.

At nonzero Δ the energy scale Δ comes into play, along with the corresponding spin rotation time $T_\Delta = 2\pi/\Delta$. Then the competition between the Zeeman field and nonlinearity determines three possible regimes, namely, for Δ smaller, larger, or of the order of the crossover value $\Delta_{cr} \equiv |\mu|$. Typical evolution patterns of the BEC parameters for the three regimes are shown respectively in Figs. 1, 2, and 3 and will be discussed in the following.

(i) Weak Zeeman field ($\Delta \ll |\mu|$, $T_\Delta \gg T_\mu$). This regime is characterized by clearly different dynamics of the two spinor components [see Fig. 1(a)], small-amplitude spin rotations, $|\sigma_x(t)|, |\sigma_y(t)| \ll 1$ (Fig. 2), and a relatively small broadening of the wave packet over time T_Δ. The latter is due to the fact that weak Zeeman fields only produce a small population of

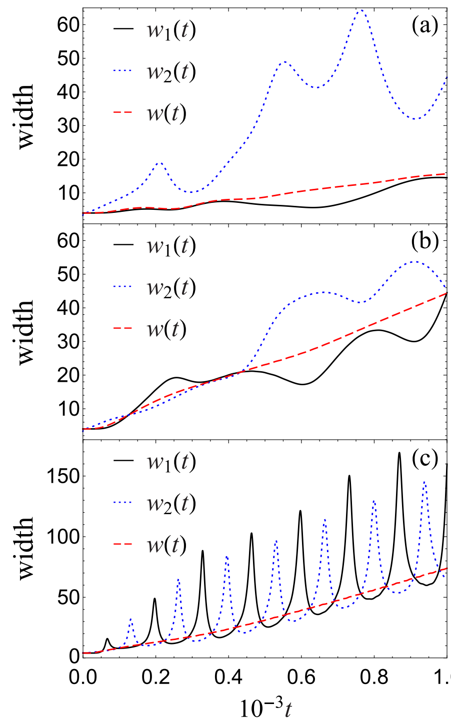

FIG. 1. Width of the free-space [$U(x) \equiv 0$] BEC for (a) $\Delta = 0.01$, (b) $\Delta = 0.02$, and (c) $\Delta = 0.05$. Here and below we use for numerical simulations $g = 0.5$.

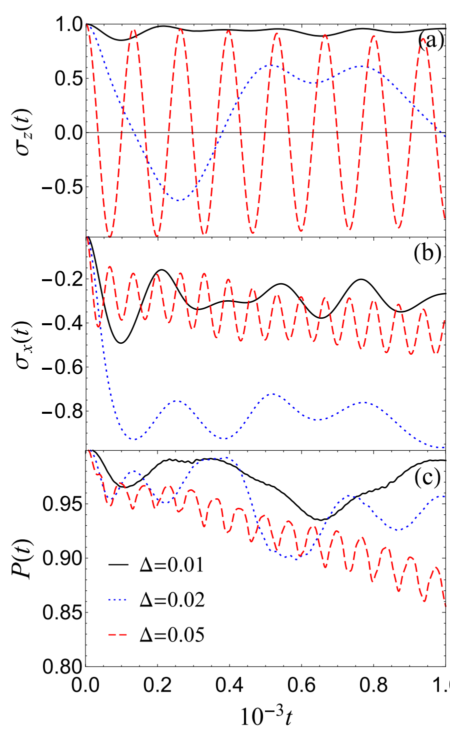

FIG. 2. Evolution of the spin components along the (a) z and (b) x axes and of (c) $P(t) = \sum_i \sigma_i^2(t)$ for a free-space BEC at $\Delta = 0.01, 0.02, 0.05$.

[1]The factor $\frac{1}{3}$ in Eq. (4) ensures that for the soliton shape in Eq. (6) one obtains $\zeta(0) = w_0$.

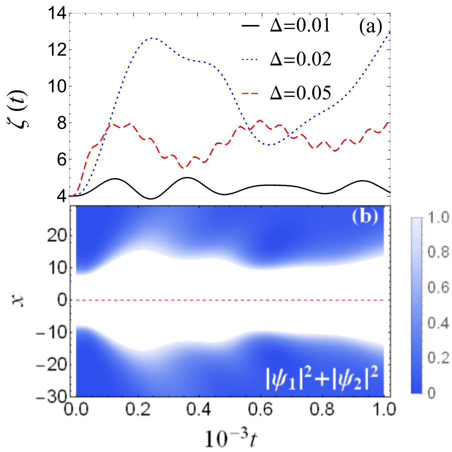

FIG. 3. (a) Participation ratio of the free-space BEC defined by Eq. (4) for $\Delta = 0.01$, 0.02, and 0.05. The broadening of the soliton with the reorientation of the spin is evident for Δ close to the crossover value $\Delta_{cr} = |\mu|$. (b) Density plot of the condensate in (t, x) space for $\Delta = 0.02$.

the second component, $N_2(t) \ll 1$, so that, even though this component spreads rapidly (with speed of the order of g, essentially due to the momentum-position uncertainty), it only produces a moderate increase of the total width w [recall that the initial state $\psi_1(x)$ is stationary]. Regarding the behavior of the spin components shown in Fig. 2, iterative solution of Eq. (1) corroborated by numerical results shows that at the initial stage $t \ll T_\mu$, $\sigma_x(t)$ behaves as $2\Delta t^2\mu/3$ and the minimum value of $\sigma_x(t)$ is of the order of Δ/μ, while the maximum value of $1 - \sigma_z(t)$ is of the order of $(\Delta/\mu)^2 \ll \max[|\sigma_x(t)|]$.

(ii) Crossover regime ($\Delta \sim |\mu|$, $T_\Delta \sim T_\mu$). The Zeeman field becomes sufficiently strong to rotate the spin by producing a sizable population $N_2(t)$. Consequently, the broadening of this component decreases due to the self-attraction. In this case, the wave-packet broadening during a spin rotation period T_Δ is of the order of w_0, and spin components which can trigger a substantial population exchange due to sufficient Zeeman energy changes, namely, $\sigma_z(t) < 0$ and $\sigma_x(t) \approx -1$, can be achieved. Here both components feature similar broadening with time while the dynamics of all relevant quantities is rather irregular. Numerical results show that although at $t > T_\Delta$ the initial soliton shape is already destroyed, its spin state remains almost pure (see Fig. 2) with $P(t) \approx 1$. Therefore, $\psi_1(\mathbf{x})$ and $\psi_2(\mathbf{x})$ still remain approximately linearly dependent and the densities $|\psi_1(\mathbf{x})|^2$ and $|\psi_2(\mathbf{x})|^2$ have similar profiles.

(iii) Strong magnetic field ($\Delta \gg |\mu|$, $T_\Delta \ll T_\mu$). In this case the two spin components show regular oscillations, with $\sigma_z(t) \approx \cos(\Delta t)$. The soliton width increases almost linearly, each component being characterized by alternating periodic kicks [see Fig. 1(c)]. These kicks are due to the fact that each component spreads rapidly when its population $N_\nu(t)$ is minimal [see the discussion in point (i)], and then, when $N_\nu(t) \approx 1$, the spread rate decreases significantly due to the self-attraction. The analysis of the energy conservation yields that at a quarter of the Zeeman period $t = T_\Delta/4$, where $|N_2(t) - N_1(t)| \ll 1$, one obtains $\sigma_x(\pi/2\Delta) \approx 2\mu/3\Delta$, corresponding to the Zeeman energy required for this rotation [cf. Fig. 2(b)].

B. Displacement driven by spin reorientation and disorder

A smooth disorder, like in the Lifshitz model [19], is produced, over large distance L, by a distribution of $\mathcal{N} \gg 1$ impurities with uncorrelated random positions x_j and mean linear density $\bar{n} = \mathcal{N}/L$ as

$$U(x) = U_0 \sum_{j=1}^{j=\mathcal{N}} s_j u(x - x_j). \qquad (7)$$

Here $s_j = \pm 1$ is a random function of j with mean values $\langle s_j \rangle = 0$, so $\langle U(x) \rangle = 0$. Here we model the impurities as $u(y) = \exp(-y^2/\xi^2)$, where ξ is the corresponding width (the results discussed in the following do not depend qualitatively on this specific choice). The motion of the BEC center of mass $X(t)$ [see Eq. (2)] is described by the Ehrenfest theorem [20] as

$$\frac{d^2X(t)}{dt^2} = F[\boldsymbol{\psi}] \equiv -\mathrm{tr}\int_{-\infty}^{\infty} \boldsymbol{\rho}(\mathbf{x})U'(x)dx, \qquad (8)$$

where $F[\boldsymbol{\psi}]$ is the state-dependent force. For random $U(x)$, we choose as the initial condition a stationary solution of Eq. (1) $\boldsymbol{\psi}^{[d]}(\mathbf{x}_0) = [\psi_1^{[d]}(\mathbf{x}_0), 0]^{\mathrm{T}}$ with $F[\boldsymbol{\psi}^{[d]}(\mathbf{x}_0)] = 0$, where $\mathbf{x}_0 \equiv (x, 0)$, corresponding to $\sigma_z(0) = 1$ as in the discussion of the free-space case.

The disorder introduces a new energy-dependent timescale of elastic momentum relaxation related to particle backscattering in a random potential. For a wave packet, this timescale, being associated with the packet width in the momentum space, determines the time of free broadening of the packet until the localization effect will become essential. In the Born scattering approximation this timescale is $\tau_d \equiv g/U_0^2\bar{n}\xi^2$ and the corresponding expansion length becomes $\ell = g\tau_d$ [21,22]. We assume that the potential is weak such that $\ell \gg 1/g$, that is, the initial width corresponding to $\psi_1^{[d]}(\mathbf{x}_0)$ [see Eq. (4)], $\zeta(0) \approx w_0$, is due to the self-interaction rather than due to the conventional Anderson localization. In the following we consider relatively weak self-interactions $g\xi \lesssim 1$ to study wave packets extended over several correlation lengths of $U(x)$, where the effect of disorder is expected to be essential. Notice that in this regime the potential is not able to localize the condensate near a single minimum of $U(x)$, that is, $\xi^2\langle U^2\rangle^{1/2} \ll 1$, where $\langle U^2\rangle = U_0^2\bar{n}\xi\sqrt{\pi}$. Also, we assume that $\min(\Delta, |\mu|)\tau_d \gtrsim 1$, hence the disorder does not influence strongly the short-term expansion.

In the following we develop a simple scaling theory, describing this process qualitatively, and then compare it with numerical results. For broad states as considered here, the force f_j imposed on the condensate by a single impurity located at the point x_j is given by

$$f_j = \sqrt{\pi}U_0 s_j \xi \partial_x |\boldsymbol{\psi}(\mathbf{x})|^2|_{x=x_j}. \qquad (9)$$

Disorder averaging $\langle F^2[\boldsymbol{\psi}]\rangle \equiv \langle(\sum_j f_j)^2\rangle$ for the entire BEC yields [19] (see the Appendix for details)

$$\langle F^2[\boldsymbol{\psi}]\rangle = \pi U_0^2\xi^2\bar{n}\int_{-\infty}^{\infty}[\partial_x|\boldsymbol{\psi}(\mathbf{x})|^2]^2dx. \qquad (10)$$

Equation (10) cannot be directly applied to the system considered here since the specific initial equilibrium condition $F[\boldsymbol{\psi}^{[d]}(\mathbf{x}_0)] = 0$ is not a subject of direct disorder averaging. Then we proceed as follows. At the initial stage of expansion ($t \ll T_\Delta$) of this strongly asymmetric set of the components we have

$$\psi_1^{[d]}(\mathbf{x}) = \psi_1^{[d]}(\mathbf{x}_0) + \delta\psi_1^{[d]}(\mathbf{x}), \quad \psi_2^{[d]}(\mathbf{x}) = \delta\psi_2^{[d]}(\mathbf{x}), \quad (11)$$

and the corresponding net force δF acting on the condensate due to the $\delta\psi_1^{[d]}(\mathbf{x})$ term is expressed as

$$\delta F = -2\,\mathrm{Re}\int_{-\infty}^{\infty} \psi_1^{[d]}(\mathbf{x}_0)\delta\psi_1^{[d]}(\mathbf{x})U'(x)dx. \quad (12)$$

For a qualitative analysis, we can use a model of expansion of $\psi_1^{[d]}(\mathbf{x})$ by assuming that the change in its shape is solely due to a change in the width δw. With the same approach to the averaging of δF, we obtain (details are presented in the Appendix)

$$\langle(\delta F)^2\rangle = \frac{7\pi^2}{90}\frac{(\delta w)^2}{w_0^2}\langle F^2[\boldsymbol{\psi}]\rangle. \quad (13)$$

Here $\langle F^2[\boldsymbol{\psi}]\rangle = \pi U_0^2\xi^2\bar{n}g^3/30$ is a consequence of Eq. (10) for the state in Eq. (6). It is applicable for the weak disorder considered here, where the equilibrium shape $\psi_1^{[d]}$ is close to $\psi_1(\mathbf{x})$ in Eq. (6). Thus, the broadening of the wave packet caused by switching on the Zeeman field results in covering a different random potential and triggers its motion.[2]

Now the three regimes of the spin evolution and broadening due to the Zeeman field $\Delta\sigma_x/2$ leading to qualitatively similar regimes of its motion in the random field can be identified. The main feature of the driven motion is that the force δF needs a certain time to develop and then it drives displacement of the condensate $X(t) - X(0)$. For $\Delta \ll |\mu|$ we have $|F[\psi_2^{[d]}(\mathbf{x})]| \ll |F[\psi_1^{[d]}(\mathbf{x})]|$, the driven variations in the density are weak, and the position shows only small irregular oscillations. At $\Delta \gtrsim |\mu|$ (crossover and strong Zeeman couplings) the contributions of $F[\psi_2^{[d]}(\mathbf{x})]$ and $F[\psi_1^{[d]}(\mathbf{x})]$ are of the same order of magnitude, scaling as $(U_0^2\xi^2\bar{n}g^3)^{1/2}$. Therefore, in the crossover regime, the displacement during one Zeeman period can be estimated from Eq. (8) as $\langle F^2\rangle^{1/2}T_\Delta^2$, that is,

$$\sqrt{\langle X^2(T_\Delta)\rangle} \sim U_0\xi\sqrt{\bar{n}}g^{-5/2}. \quad (14)$$

The condition for a large displacement during T_Δ triggering a long-distance propagation of the condensate corresponds to $\sqrt{\langle X^2(T_\Delta)\rangle} \sim w_0$, that is, $U_0\xi\sqrt{\bar{n}}g^{-3/2} \gtrsim 1$. The subsequent motion is a manifestation of the spin-position coupling due to the non-Manakov self-interaction in the BEC that can appear without SOC.

For numerical calculations, in the following we set $\xi = 1$, $\bar{n} = 10/\xi$, and $U_0 = 0.01$. With this choice, the ground state of the condensate extends over several disorder correlation lengths, that is, $2/g \gg \xi$ (we recall that $g \equiv 0.5$). Figure 4

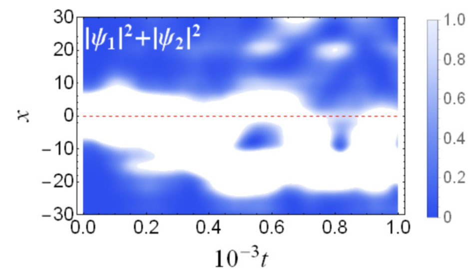

FIG. 4. Density plot of the condensate in a random potential for $\Delta = 0.02$. The initial values of the center-of-mass position and of the condensate width are $X(0) \simeq 0.19$ and $\zeta(0) \simeq 3.25$, respectively. Note that for $t < 100$ ($t < \tau_d$) this plot is very similar to that in Fig. 3(b).

shows a typical evolution of the total density and demonstrates the net displacement and the change in the shape of the condensate, including its possible splitting between two potential minima. The spin evolution as presented in Fig. 5 shows that the purity of the spin state $P(t)$ is rapidly destroyed by the random potential due to the fact that $\psi_1^{[d]}(\mathbf{x})$ and $\psi_2^{[d]}(\mathbf{x})$ are linearly independent.

The evolution of the force acting on the wave packet, its size, and position are presented in Fig. 6. This figure show that in a weak Zeeman field the condensate displacement is much smaller than its width, the forces are weak, and the change in the width is small. Thus, the condensate shows only small irregular oscillations near $X(0)$, as expected. Figure 6(b) clearly demonstrates that, also in the presence of disorder, broadening of the soliton depends on the Zeeman field. The

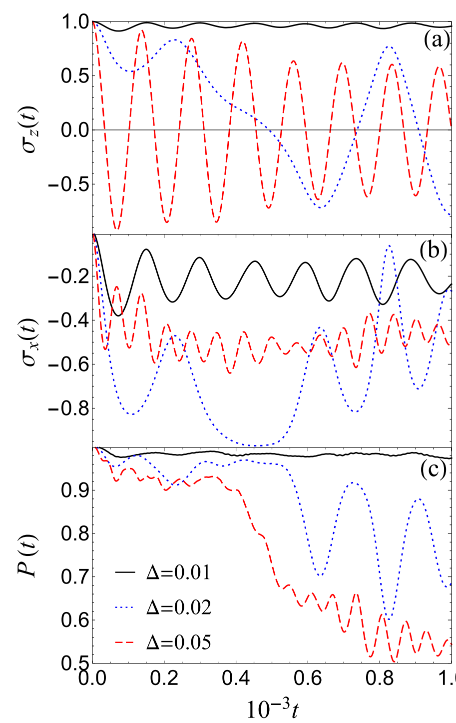

FIG. 5. Evolution of the spin components along the (a) x and (b) x axes and (c) of $P(t)$ for $\Delta = 0.01$, 0.02, and 0.05 (solid, dotted, and dashed lines, respectively).

[2]Note that for a zero-width potential with $\xi \to 0$, the force vanishes even if the mean value of $\langle U^2\rangle$ is still finite. Therefore, in this limit $X(t) = X(0)$.

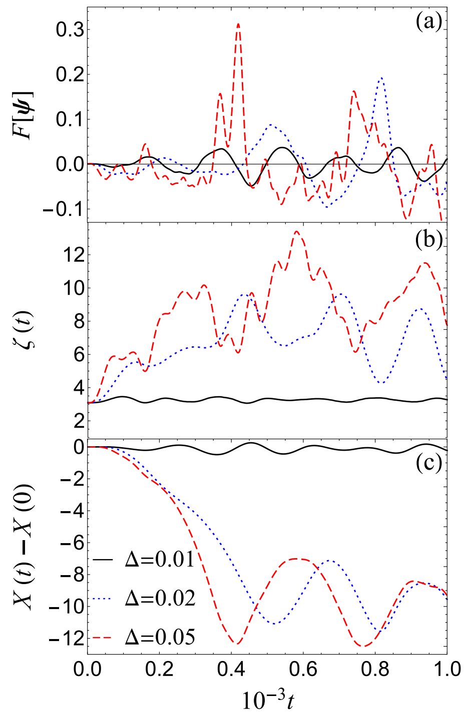

FIG. 6. Evolution of (a) the state-dependent force defined by Eq. (10), (b) the participation ratio, and (c) the displacement of the center of mass $X(t)-X(0)$ for different values of Δ.

forces presented in Fig. 6(a) have a clear correlation with the quantities shown in Figs. 6(b) and 6(c). Indeed, the force is large when ζ is small and d^2X/dt^2 is large at large F. In addition, a comparison with the multipeak density profile in Fig. 4 confirms that the force is determined by $\zeta(t)$ in Eq. (4) rather than by the total spread $w(t)>\zeta(t)$ in Eq. (5). Although the random motion considerably depends on the realization of $U(x)$, this dependence is only quantitative, and the entire qualitative analysis remains valid independent of the given realization.

Having discussed a realization with $\tilde{g}=0$ and single-component initial conditions, we proceed with a brief analysis of other possible scenarios. We begin with the same initial condition and different $\tilde{g}$, as presented in Fig. 7, demonstrating that with the increase in $\tilde{g}$, the driving effect of the Zeeman field decreases and vanishes for the SU(2) symmetry [23–25], where $\tilde{g}=g$. In this limit, the spin rotation does not require energy to modify the self-interaction since the

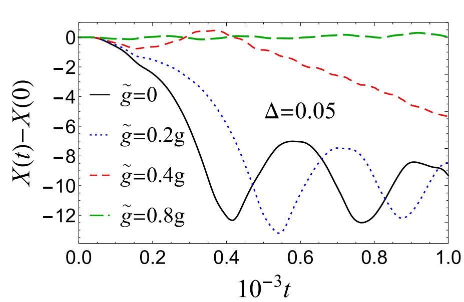

FIG. 7. Time-dependent displacement of the center of mass for different values of $\tilde{g}$ and $\Delta=0.05$.

condensate rotates without change in its shape as $\boldsymbol{\psi}^{[d]}(\mathbf{x})=\psi_1^{[d]}(\mathbf{x}_0)[\cos(\Delta t/2),\sin(\Delta t/2)]^{\mathsf{T}}$ and no net force δF appears as a result. As far as the role of the initial conditions is concerned, we notice that there is an infinite number of states $\boldsymbol{\psi}^{[d]}(\mathbf{x}_0)=[\psi_1^{[d]}(\mathbf{x}_0),\psi_2^{[d]}(\mathbf{x}_0)]^{\mathsf{T}}$ satisfying the stationarity condition $F[\boldsymbol{\psi}^{[d]}(\mathbf{x}_0)]=0$. When a Zeeman field is applied along the x axis, a precession around this axis begins, which in turn modifies the density distribution, then leading to a nonzero force and causing further dynamics. For linearly independent $\psi_1^{[d]}(\mathbf{x}_0)$ and $\psi_2^{[d]}(\mathbf{x}_0)$, the spin rotation leads to a change in the self-interaction energy, and in general a net force appears for the SU(2) coupling as well. This guarantees that the triggering of the motion of an initially stationary BEC by a Zeeman field as discussed in the present paper is in fact a general feature of self-interacting pseudospin-$\frac{1}{2}$ condensates.

IV. CONCLUSION

We have demonstrated that the motion of the center of mass of a self-attractive spinor Bose-Einstein condensate can be caused by the joint effect of the spin precession in a Rabi-like Zeeman field and the presence of an external potential considered here in a random form as an example. The broadening of the condensate caused by the spin rotation leads to a net force acting on it and triggers its motion. Thus, the spin evolution can drive changes in the condensate position even in the absence of spin-orbit coupling. These results hint at possible interesting extensions of the present study, including the theory of multidimensional and multisoliton settings.

ACKNOWLEDGMENTS

We acknowledge support from the Spanish Ministry of Economy, Industry and Competitiveness (MINECO) and the European Regional Development Fund FEDER through Grant No. FIS2015-67161-P (MINECO/FEDER, UE) and the Basque Government through Grant No. IT986-16. S.M. was partially supported by the Swiss National Foundation SCOPES Project No. IZ74Z0-160527. The work of B.A.M. was supported in part by the Binational (U.S.-Israel) Science Foundation through Project No. 2015616 and by the Israel Science Foundation through Grant No. 1286/17. We are grateful to V. V. Konotop and Y. V. Kartashov for discussions and valuable comments.

APPENDIX: DISORDER AVERAGING

Here we describe the disorder-averaging calculation of the force acting on the condensate in a random field. For the definiteness, we omit the time dependence and consider only the relevant coordinate dependences using the same notation as in the main text.

We consider a random potential produced by the distribution of impurities with white-noise uncorrelated random positions x_j and mean linear density $\bar{n}$ of the

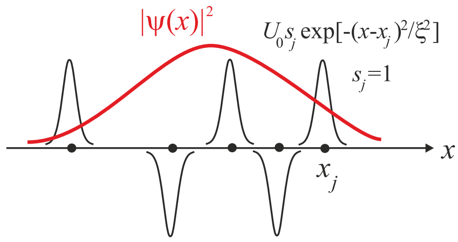

FIG. 8. Schematic plot of the BEC density $|\psi(x)|^2$ and impurity potential. Positions of impurities are marked with closed circles.

form

$$U(x) = U_0 \sum_j s_j u(x - x_j), \tag{A1}$$

where $s_j = \pm 1$ is a random function of j with mean value $\langle s_j \rangle = 0$, so that $\langle U(x) \rangle = 0$, and the Gaussian shape $u(x - x_j) = \exp[-(x - x_j)^2/\xi^2]$, where ξ is the corresponding width. We begin with the effect of a single impurity located at the point x_j on the condensate energy and applied force for broad states of our interest (see Fig. 8). The single-impurity interaction energy v_j and force f_j are given by

$$v_j = U_0 s_j \int_{-\infty}^{\infty} |\psi(x)|^2 u(x - x_j) dx, \tag{A2}$$

$$f_j = -U_0 s_j \int_{-\infty}^{\infty} |\psi(x)|^2 u'(x - x_j) dx. \tag{A3}$$

For the chosen Gaussian impurity shape we obtain

$$v_j = \sqrt{\pi} U_0 s_j \xi |\psi(x_j)|^2. \tag{A4}$$

For the force we expand the density in the vicinity of the x_j point as $|\psi(x)|^2 = |\psi(x_j)|^2 + [d|\psi(x)|^2/dx]|_{x=x_j}(x - x_j)$ and obtain

$$f_j = \sqrt{\pi} U_0 s_j \xi \frac{d}{dx} |\psi(x)|^2 \bigg|_{x=x_j}. \tag{A5}$$

To produce the disorder averaging for the uncorrelated distribution of impurities, $\langle F^2[\psi] \rangle \equiv \langle (\sum_j f_j)^2 \rangle$ and $\langle V^2[\psi] \rangle \equiv \langle (\sum_j v_j)^2 \rangle$ for the entire condensate, we use the technique presented in detail in Ref. [19]. With this approach the sum over impurities for a function $\chi(x)$, $p_\chi \equiv \sum_j \chi(x_j)$, is presented as an integral, in our case in the form

$$\langle p_\chi^2 \rangle = \bar{n} \int \delta(x - x') \chi(x) \chi(x') dx\, dx'. \tag{A6}$$

Thus, we arrive at the transformation

$$\langle p_\chi^2 \rangle = \bar{n} \int \chi^2(x) dx \tag{A7}$$

and obtain for the energy and force

$$\langle V^2[\psi] \rangle = \pi U_0^2 \xi^2 \bar{n} \int_{-\infty}^{\infty} |\psi(x)|^4 dx$$
$$= \frac{\pi}{3} U_0^2 \xi^2 \bar{n} \frac{1}{\zeta}, \tag{A8}$$

$$\langle F^2[\psi] \rangle = \pi U_0^2 \xi^2 \bar{n} \int_{-\infty}^{\infty} \left(\frac{d}{dx} |\psi(x)|^2 \right)^2 dx, \tag{A9}$$

where the participation ratio ζ is defined by Eq. (4). For the wave function in Eq. (6),

$$\psi_1(x) = \frac{\text{sech}(x/w_0)}{\sqrt{2w_0}}, \quad \psi_2(x) = 0, \tag{A10}$$

these equations yield

$$\langle V^2[\psi] \rangle = \frac{\pi}{6} U_0^2 \xi^2 \bar{n} g, \tag{A11}$$

$$\langle F^2[\psi] \rangle = \frac{\pi}{30} U_0^2 \xi^2 \bar{n} g^3. \tag{A12}$$

Note that these relations can readily be understood by using the basic fluctuations theory for noncorrelated ensembles. For this purpose we recall that the relevant spatial scale of the BEC density distribution is ζ. Then, for a qualitative scaling analysis, the fluctuations in $V[\psi]$ and $F[\psi]$ can be presented in terms of the difference in the number of impurities with $s_j = 1$ and $s_j = -1$ at this spatial scale. The fluctuation of the square of this difference, relevant for $\langle V^2[\psi] \rangle$ and $\langle F^2[\psi] \rangle$, is of the order $\bar{n}\zeta$, which yields $\langle V^2[\psi] \rangle \sim U_0^2 \xi^2 \bar{n}/\zeta$ and $\langle F^2[\psi] \rangle \sim U_0^2 \xi^2 \bar{n}/\zeta^3$, in agreement with Eqs. (A11) and (A12).

The above disorder-averaging procedure of the force is not directly applicable near the equilibrium since at $t = 0$ a special condition $F[\psi^{[d]}(x)] = 0$ is satisfied. Thus, we have to consider variation of the force δF due to the variations of the BEC wave function in the form

$$\delta F = -2\,\text{Re} \int_{-\infty}^{\infty} \psi_1^{[d]}(x_0) \delta \psi_1^{[d]}(x) U'(x) dx. \tag{A13}$$

Due to a change in the width δw, this variation for the wave function in Eq. (6) becomes

$$\delta \psi_1^{[d]}(x) = \delta w \frac{x \sinh(x/w_0)}{\sqrt{2} w_0^{5/2} \cosh^2(x/w_0)} \tag{A14}$$

and we arrive at Eq. (13), with $\langle F^2[\psi] \rangle$ from Eq. (A12).

[1] S. Flach, D. O. Krimer, and C. Skokos, Phys. Rev. Lett. **102**, 024101 (2009).

[2] I. L. Aleiner, B. L. Altshuler, and G. V. Shlyapnikov, Nat. Phys. **6**, 900 (2010).

[3] E. Lucioni, B. Deissler, L. Tanzi, G. Roati, M. Zaccanti, M. Modugno, M. Larcher, F. Dalfovo, M. Inguscio, and G. Modugno, Phys. Rev. Lett. **106**, 230403 (2011).

[4] B. W. A. Leurs, Z. Nazario, D. I. Santiago, and J. Zaanen, Ann. Phys. (NY) **323**, 907 (2008).

[5] J. Schliemann, D. Loss, and R. M. Westervelt, Phys. Rev. Lett. **94**, 206801 (2005).

[6] W. Zawadzki, Phys. Rev. B **72**, 085217 (2005).
[7] R. Winkler, U. Zülicke, and J. Bolte, Phys. Rev. B **75**, 205314 (2007).
[8] H. Zhai, Int. J. Mod. Phys. B **26**, 1230001 (2012).
[9] V. Galitski and I. B. Spielman, Nature (London) **494**, 49 (2013).
[10] L. Wen, Q. Sun, Y. Chen, D.-S. Wang, J. Hu, H. Chen, W.-M. Liu, G. Juzeliūnas, B. A. Malomed, and A.-C. Ji, Phys. Rev. A **94**, 061602(R) (2016).
[11] I. M. Uzunov, R. Muschall, M. Gölles, Y. S. Kivshar, B. A. Malomed, and F. Lederer, Phys. Rev. E **51**, 2527 (1995).
[12] B. A. Malomed, in *Handbook of Optical Fibers*, edited by G.-D. Peng (Springer Nature, Singapore, 2018).
[13] J. Williams, R. Walser, J. Cooper, E. A. Cornell, and M. Holland, Phys. Rev. A **61**, 033612 (2000).
[14] A. Sartori, J. Marino, S. Stringari, and A. Recati, New J. Phys. **17**, 093036 (2015).
[15] H. Saito, R. G. Hulet, and M. Ueda, Phys. Rev. A **76**, 053619 (2007).
[16] H. Susanto, P. G. Kevrekidis, B. A. Malomed, and F. K. Abdullaev, Phys. Lett. A **372**, 1631 (2008).
[17] A. Mostofi, B. A. Malomed, and P. L. Chu, Opt. Commun. **145**, 274 (1998).
[18] S. V. Manakov, Zh. Eksp. Teor. Fiz. **65**, 505 (1973) [Sov. Phys. JETP **38**, 248 (1974)].
[19] For the averaging technique, see A. L. Efros and B. I. Shklovskii, *Electronic Properties of Doped Semiconductors* (Springer, Heidelberg, 1989).
[20] P. Ehrenfest, Z. Phys. **45**, 455 (1927).
[21] L. P. Gor'kov, in *Electron-Electron Interactions in Disordered Systems*, edited by A. L. Efros and M. Pollak (North-Holland, Amsterdam, 1985).
[22] For momentum relaxation in two-dimensional random optical potentials, see J. Richard, L.-K. Lim, V. Denechaud, V. V. Volchkov, B. Lecoutre, M. Mukhtar, F. Jendrzejewski, A. Aspect, A. Signoles, L. Sanchez-Palencia, and V. Josse, arXiv:1810.07574.
[23] I. V. Tokatly and E. Ya. Sherman, Ann. Phys. (NY) **325**, 1104 (2010).
[24] I. V. Tokatly and E. Y. Sherman, Phys. Rev. A **87**, 041602 (2013).
[25] Note that the effect of $\tilde{g}$ on the wave-packet spread is somewhat analogous to spin drag in fermionic systems; See I. D'Amico and G. Vignale, Phys. Rev. B **62**, 4853 (2000); M. Polini and G. Vignale, Phys. Rev. Lett. **98**, 266403 (2007); R. A. Duine, M. Polini, H. T. C. Stoof, and G. Vignale, *ibid.* **104**, 220403 (2010).